Reconsidering the *czcD* (NiCo) Riboswitch as an Iron Riboswitch

Jiansong Xu and Joseph A. Cotruvo, Jr.*

Cite This: *ACS Bio Med Chem Au* 2022, 2, 376−385
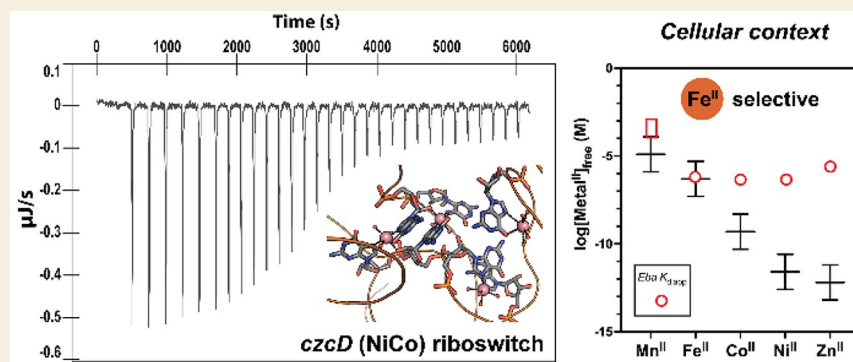
Read Online

ACCESS | Metrics & More | Article Recommendations | SI Supporting Information

ABSTRACT: Recent work has proposed a new mechanism of bacterial iron regulation: riboswitches that undergo a conformational change in response to Fe^{II}. The *czcD* (NiCo) riboswitch was initially proposed to be specific for Ni^{II} and Co^{II}, but we recently showed via a *czcD*-based fluorescent sensor that Fe^{II} is also a plausible physiological ligand for this riboswitch class. Here, we provide direct evidence that this riboswitch class responds to Fe^{II}. Isothermal titration calorimetry studies of the native *czcD* riboswitches from three organisms show no response to Mn^{II}, a weak response to Zn^{II}, and similar dissociation constants (∼1 μM) and conformational responses for Fe^{II}, Co^{II}, and Ni^{II}. Only the iron response is in the physiological concentration regime; the riboswitches' responses to Co^{II}, Ni^{II}, and Zn^{II} require 10^3-, 10^5-, and 10^6-fold higher "free" metal ion concentrations, respectively, than the typical availability of those metal ions in cells. By contrast, the "Sensei" RNA, recently claimed to be an iron-specific riboswitch, exhibits no response to Fe^{II}. Our results demonstrate that iron responsiveness is a conserved property of *czcD* riboswitches and clarify that this is the only family of iron-responsive riboswitch identified to date, setting the stage for characterization of their physiological function.

KEYWORDS: Irving-Williams series, metalloregulation, RNA, iron overload, metal selectivity, metal sensor

INTRODUCTION

Life has long wrestled with the beneficial and deleterious catalytic potential of iron. The ubiquity of Fe^{II} in the early earth has led to proposals that it played important roles in prebiotic chemistry[1−4] and in hydrolysis and electron transfer chemistry in the hypothesized RNA world.[5,6] Through the utility of its Lewis acidity, the $Fe^{II,III}$ redox couple, its assembly into more complex cofactors such as iron−sulfur clusters[7,8] and heme,[9] and its facile reactivity with O_2,[10] the chemistry of iron has found its way into many of the core metabolic reactions of nearly every known extant organism.[11] At the same time, however, iron also catalyzes destructive radical chemistry under oxic conditions, which may result in oxidative stress if improperly regulated;[12−14] the possibility that high iron levels also may be toxic under anoxic conditions is tantalizing but has been less explored.[4,15]

Bacterial metalloregulatory systems for iron and other metal ions selectively sense the bioavailable (also called labile or "free") concentrations of metal ions and control the expression of proteins involved in metal ion uptake, efflux, storage, and utilization, to maintain cellular free metal ion concentrations within a narrow range.[16−18] On the basis of numerous studies and across several organisms,[19−25] this range for iron appears to be high nanomolar to low micromolar. Iron is maintained at a relatively high labile concentration because its affinity for biological ligands tends to be relatively low, according to the Irving-Williams (IW) series, which ranks the affinities of metal−ligand complexes of divalent metal ions: $Mg^{II} < Mn^{II} < Fe^{II} < Co^{II} < Ni^{II} < Cu^{II} > Zn^{II}$.[26] This trend dictates the relative buffered concentration ranges and consequently the affinities of the metalloregulators for each metal ion, spanning tens of micromolar for Mn^{II}, low micromolar for Fe^{II}, to picomolar for Zn^{II} and attomolar for copper (Cu^I).[18]

Importantly, the fidelity of the regulators for metals low in the IW series, such as the ferric uptake regulator (Fur) for Fe^{II}, is frequently not the result of that regulator being highly specific for that metal;[27] in fact, Fur binds Co^{II} and Zn^{II} with higher affinity than Fe^{II} in vitro.[20] Instead, the cell maintains low labile concentrations of the metals higher in the IW series, thereby ensuring that the bioavailable concentrations of the high-IW metals are too low to aberrantly activate the low-IW regulator under most conditions.[24,25]

Within this framework, bacteria often possess different regulators to sense deficiency and excess of a particular metal ion. For example, Zn^{II} deficiency and excess are sensed by two different transcription factors (Zur and ZntR) that regulate Zn^{II} importers and exporters/storage, respectively.[16] Mn^{II} levels are controlled by a transcription factor (MntR), regulating uptake and export, and riboswitches—RNA elements, located in the 5′-untranslated regions (5′-UTRs) of genes, which bind ligands to cause a conformational change to alter transcription or translation of the downstream gene[28−30]—as sensors of manganese excess, regulating the expression of Mn^{II} efflux proteins.[31−33] In the case of iron, characterized regulators such as Fur[20] are primarily charged with sensing deficiency or sufficiency, either directly as a repressor or as activator via the small antisense RNA, *ryhB*.[34] Only recently have studies identifying iron-exporting ATPases pointed to the relevance of iron excess in bacteria under aerobic conditions[35−37] and its intriguing links to pathogenesis.[38−40] However, there is little understanding of mechanisms of toxicity and sensing of iron excess, and particularly whether they extend to anaerobic conditions, where oxidative stress is unlikely.[41]

Two recent publications have proposed riboswitches as an additional mechanism of sensing iron in bacteria. [Like the bacterial riboswitches, eukaryotic iron-responsive elements (IREs) may also sense iron by direct Fe^{II} binding.[42]] In 2020,[43] we reported evidence that the *czcD* or "NiCo" riboswitch could respond to iron. This riboswitch is found in a number of obligate and facultative anaerobes, many of which are associated with the human gut as commensals and/or are human pathogens, such as *Erysipelotrichaceae bacterium* (*Eba*; this riboswitch was crystallographically characterized with Co^{II} bound[44]), *Listeria monocytogenes* (*Lmo*), *Enterococcus faecium*, *Clostridium botulinum*, and other nonpathogenic clostridioides such as *C. cellulolyticum* (*Cce*). In 2015, the *czcD* riboswitch had been initially characterized as responsive to Ni^{II} and Co^{II} by Breaker, Winkler, and co-workers and was proposed to sense cobalt and nickel excess and regulate putative efflux proteins.[44] We hypothesized that Fe^{II} binding to this riboswitch had been overlooked, because those studies had been performed under aerobic conditions, in which Fe^{II} rapidly oxidizes to insoluble Fe^{III}.[43] Indeed, we showed that fluorescent sensors constructed from the *Eba* riboswitch respond to Fe^{II} (as well as to Co^{II}, Ni^{II}, and other divalent first-row transition metals), and one of these sensors also responded to iron when expressed in *Escherichia coli*. Furthermore, the genes regulated by the *Eba* and *Lmo* riboswitches rescued iron toxicity when expressed in *Bacillus subtilis*, presumably by mediating Fe^{II} efflux. Therefore, although our in vitro studies were conducted with the *czcD*-based sensor, we proposed that the native *czcD* riboswitch itself might be iron-responsive in vivo.

A subsequent report from Ramesh and co-workers,[45] premised on the nonresponsiveness of *czcD* to Fe^{II}, used bioinformatic methods to identify putative riboswitches that would be similar to *czcD* but would bind Fe^{II} instead of Co^{II} and Ni^{II}. The RNAs identified, dubbed "Sensei," were proposed to be structurally similar to *czcD* riboswitches. Isothermal titration calorimetry (ITC) studies suggested that the Sensei RNA from *Haemophilus ducreyi* (*Hdu*) was conformationally responsive to Fe^{II} but not Co^{II}. Their claim that both *czcD* and Sensei were *specific* for their proposed ligands—Co^{II}/Ni^{II} and Fe^{II}, respectively—was surprising, because it conflicted with the understanding of metal-loregulation presented above, implying that metal selectivity rules differ for RNA and protein regulators.

Here, using two independent approaches, riboswitch-based fluorescent sensors and ITC, we demonstrate that *czcD* riboswitches from three organisms undergo a similar conformational change to Fe^{II} as to Co^{II} and Ni^{II}, all with similar apparent dissociation constants (0.5−2 μM). These results demonstrate that iron responsiveness is a general property of the *czcD* family, and we propose that iron is the most likely cellular ligand for these riboswitches. By contrast, the Sensei RNA does not respond to Fe^{II} or Co^{II}. These results establish the *czcD* riboswitch as the only known family of iron-responsive riboswitches, support a unified framework for protein- and RNA-based metalloregulation, and suggest a new player in the physiology of iron in numerous bacteria relevant to human health and disease.

■ EXPERIMENTAL SECTION

General Considerations

Chemical reagents were obtained from Thermo Fisher Scientific or Millipore Sigma, unless noted otherwise. Primers and gBlocks were ordered from Integrated DNA Technologies (IDT). Reagents used for PCR amplification and RNA transcription (NTPs, dNTPs, Q5 DNA polymerase, OneTaq DNA polymerase, T7 RNA polymerase) were obtained from New England Biolabs. The Sequagel reagents used for urea polyacrylamide gel electrophoresis were purchased from National Diagnostics. DFHBI-1T was purchased from Tocris. PCR cleanup kits were from Omega Bio-Tek. All riboswitch and sensor constructs used in this study are listed in Table S1. All primers used to generate the riboswitches and riboswitch-based sensors are listed in Table S2.

Nucleic acid UV−visible absorption spectra were obtained on a Mettler Toledo UV5Nano. Well plate analyses (for the **Lmo** sensors) were carried out using a BioTek Synergy H1 microplate reader. Experiments utilizing Fe^{II} were conducted within a vinyl anaerobic chamber (Coy Lab Products, used for ITC studies) or an MBraun Unilab anaerobic box (used for sensor studies). All glassware was acid-washed with TraceMetal-grade nitric acid (Fisher) followed by extensive rinsing with filtered ddH_2O prior to use. All buffers were treated with Bio-Rad Chelex 100 resin (prior to metal addition) and sterile filtered. Aerobic and anaerobic isothermal calorimetry titration experiments were conducted using a TA Instruments Affinity ITC system.

Lmo Sensor Construction and Characterization

RNA sensor template library generation, screening, and citrate-buffered metal titrations were conducted as described (Table S3).[43] Buffer conditions for titrations were 30 mM MOPS, 100 mM KCl, 3 mM $MgCl_2$, 1 mM citrate, pH 7.2, and experiments were carried out at 20 °C.

Isothermal Titration Calorimetry

RNA samples were transcribed and gel-purified as described.[43] In a typical experiment, the transcription reaction was carried out on a 1.5 mL scale to afford enough RNA for three titrations at a ∼10 μM final RNA concentration. After the overnight crush-soak, the buffer containing RNA was decanted and concentrated using a 10 000

Figure 1. (A) Sequence alignment of the *Eba*, *Lmo*, and *Cce* riboswitch constructs used in this study. Metal ligands are indicated with a red inverse caret (∨). (B) X-ray crystal structure of the *Eba* riboswitch with Co^{II} ions bound (PDB code 4RUM). Metal-binding nucleotides are numbered according to Figure 1A, and Co^{II} ions are shown as salmon spheres. The occupancy of C4 (anomalous signal 5σ) was significantly lower than that of C1, C2, and C3 (anomalous signals ∼12σ).[44] Reprinted with permission from Xu and Cotruvo,[43] copyright 2020 American Chemical Society. (C) Fluorescence response of **Lmo-1** to first-row transition metal ions, with free metal concentrations buffered with 1 mM citrate. Full details and parameters from fits to the Hill equation (one set of sites) are given in Table 1.

MWCO Amicon Ultra centrifugal filtration device, followed by two cycles of 15× dilution and concentration with Buffer A (30 mM MOPS, 100 mM KCl, 3 mM MgCl$_2$, pH 7.2) using the same centrifugal filter, to exchange out of the crush-soak buffer. The resulting RNA sample (1.5 mL) was transferred into a Thermo-Scientific Slide-A-Lyzer gamma-irradiated dialysis cassette (10 000 MWCO) and dialyzed in a 275−300× volume of Buffer A for 3−4 h. After dialysis, the RNA concentration was measured, and the RNA sample was refolded as described.[43] This procedure yielded RNA concentrations of approximately 10 μM. The buffer following dialysis was used for blank runs of the ITC experiment, and all metal stocks for the ITC syringe were made using this buffer. Titrations of the metal stock solutions into the blank buffer generated minimal heats (<0.03 μJ/s per injection), and these heats were subtracted from the riboswitch titration data. Titrations with Mn^{II} (manganese(II) chloride tetrahydrate, >99%), Co^{II} (cobalt(II) chloride hexahydrate, >99%), Ni^{II} (nickel(II) chloride hexahydrate, >99%), and Zn^{II} (zinc(II) sulfate heptahydrate, >99%) were carried out aerobically. Titrations with Fe^{II} (iron(II) ammonium sulfate hexahydrate, >99%) were carried out anaerobically, in which case both the RNA sample and the dialysis buffer were deoxygenated by three cycles of degassing and refilling with nitrogen on a Schlenk line, and they were brought into the anaerobic chamber for RNA concentration measurement, metal stock preparation, and the ITC experiment. The concentrations of the metal ion solutions loaded into the ITC syringe were 600 μM for *Eba* and *Cce* titrations and 400 μM for *Lmo* titrations. The first injection was 0.1 μL (disregarded in data analysis), followed by 30 × 1.2 μL injections. Equilibration times were 180 s between injections, except for injections #2−6, which were 240 s. The sample cell was stirred at 125 rpm. The temperature was 20 °C. Samples in the autosampler were kept at 4 °C.

ITC data were analyzed using TA Instrument's NanoAnalyze software. In order to remove the contribution from nonspecific metal−RNA interactions, the baseline value at saturating metal concentrations was first subtracted from the integrated heats for each

titration, before fitting the corrected data using the "Independent" (one set of equivalent binding sites) ITC model to calculate binding parameters. As discussed below, the validity of the assumption that the baseline represents nonspecific metal binding is supported by the similarity between the magnitude of these heats and those observed for the nonresponsive M3 *Eba* riboswitch variant.

■ RESULTS

Characterization of Fluorescent Sensors Based on the *Lmo czcD* Riboswitch

Determining the cognate metal ion of a regulator like the *czcD* riboswitch is challenging, because the tightest-binding metal ion is frequently not the physiologically relevant one. With iron, there is the added practical complication that Fe^{II} is readily oxidized under aerobic conditions. Furthermore, many of the typical methods to study conformational changes of RNAs are not easily adapted to anaerobic conditions. Therefore, to assess *czcD* riboswitch−metal ion interactions in our previous study,[43] we constructed *Eba czcD* riboswitch-based fluorescent sensors by fusing the Spinach2 aptamer with the *Eba* riboswitch via its P1 stem (Figure S1C). The approach of fusion to Spinach2 has been used to generate fluorescent sensors from other riboswitches with minimal perturbation of function.[46−48] The sensors bind metal and undergo a conformational change to bind (5Z)-5-[(3,5-difluoro-4-hydroxyphenyl)methylene]-3,5-dihydro-2-methyl-3-(2,2,2-trifluoroethyl)-4*H*-imidazol-4-one (DFHBI-1T),[49] an analogue of the green fluorescent protein chromophore, leading to fluorescence activation. Our three sensors, **czcD-1**, **czcD-2**, and **czcD-3**, exhibited apparent binding affinities for divalent first-row transition metals, including Fe^{II} in an anaerobic-plate-reader-based assay, in accordance with the IW series.

Table 1. Fluorescence Response of Lmo-1 to First-Row Transition Metal Ions[a]

	Mn[II]	Fe[II]	Co[II]	Ni[II]	Zn[II]
$K_{d,app}$ (μM)[b]	N.R.[b]	3.1 ± 0.3	0.58 ± 0.05	0.17 ± 0.03	N.R.
F_{max}/F_{min}	N.D.[c]	12.3	8.0	5.3	N.D.
Hill coefficient (n)	N.D.	2.9 ± 0.4	2.2 ± 0.2	2.0 ± 0.3	N.D.

[a]See Figure 1C. [b]N.R.: No response detected. [c]N.D.: Not determined. Conditions: 30 mM MOPS, 100 mM KCl, 3 mM MgCl$_2$, 1 mM citrate pH 7.2, 20 °C; 100 nM **Lmo-1**, 10 μM DFHBI-1T.
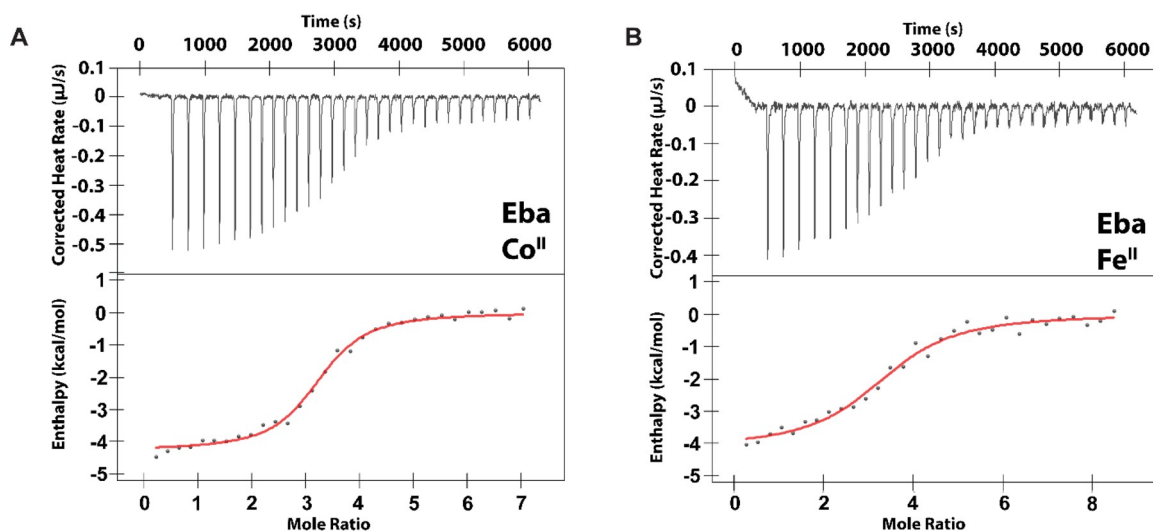
Figure 2. Representative thermograms from ITC studies of the *Eba czcD* riboswitch (8.4−9.2 μM RNA) with Co[II] (A) or Fe[II] (B). The data are fitted to a model with one set of equivalent binding sites. Fitted parameters are provided in Table 2. Conditions: 30 mM MOPS, 100 mM KCl, 3 mM MgCl$_2$, pH 7.2, 20 °C.

Table 2. Thermodynamic Parameters for Metal Ion Binding to *Eba*, *Eba* Variants, *Lmo*, and *Cce* Riboswitches, Assessed by ITC

riboswitch	metal ion	$K_{d,app}$ (μM)	n	ΔH (kcal/mol)	ΔS (cal/mol·K)
Eba	Mn[II]	N.R.[a]	N.D.[b]	N.D.	N.D.
	Fe[II]	0.99 ± 0.11	3.2 ± 0.3	−4.2 ± 0.3	12.3 ± 2.4
	Co[II]	0.57 ± 0.15	3.2 ± 0.2	−4.1 ± 0.3	14.5 ± 1.6
	Ni[II]	0.45 ± 0.14	3.3 ± 0.1	−4.1 ± 0.3	14.6 ± 1.2
	Zn[II]	2.70 ± 0.71	3.5 ± 0.8	−3.2 ± 0.3	16.1 ± 1.3
Eba-CG	Co[II]	0.88 ± 0.14	3.2 ± 0.4	−5.0 ± 0.2	10.7 ± 0.8
Eba-UA	Co[II]	0.70 ± 0.20	3.2 ± 0.3	−4.9 ± 0.3	11.3 ± 2.0
Lmo	Mn[II]	N.R.	N.D.	N.D.	N.D.
	Fe[II]	2.21 ± 0.29	1.8 ± 0.1	−6.2 ± 0.7	4.8 ± 2.4
	Co[II]	1.97 ± 0.32	2.3 ± 0.1	−6.1 ± 0.4	5.3 ± 1.5
	Ni[II]	1.20 ± 0.50	2.9 ± 0.1	−4.5 ± 0.6	12.0 ± 1.4
	Zn[II]	1.96 ± 0.13	3.0 ± 0.5	−2.5 ± 0.6	17.4 ± 2.0
Cce	Fe[II]	1.24 ± 0.12	4.8 ± 0.5	−2.7 ± 0.2	18.0 ± 0.6
	Co[II]	1.22 ± 0.18	4.5 ± 0.4	−4.2 ± 0.4	12.8 ± 1.0

[a]N.R.: No response detected. [b]N.D.: Not determined. Conditions: 30 mM MOPS, 100 mM KCl, 3 mM MgCl$_2$, pH 7.2, 20 °C; 8−15 μM riboswitch, titrated with 400 μM (*Lmo*) or 600 μM (*Eba*, variants, and *Cce*) of each metal ion.

The *czcD* riboswitch from the human pathogen, *Listeria monocytogenes* (*Lmo*), retains all of the metal-binding nucleotides of the *Eba* riboswitch (Figure 1A,B). To probe the potential iron responsiveness of this riboswitch and to establish whether attachment at P1 is a general strategy to create sensors from this family of riboswitches, here we used the same approach of Spinach2 fusion to generate three *Lmo* riboswitch-based sensors, **Lmo-1**, **Lmo-2**, and **Lmo-3**. The numerical designation refers to the number of base pairs of the P1 stem in the original riboswitch retained in the sensor. Because the Spinach2 aptamer is expected to contribute four base pairs to the stem, **Lmo-1** is anticipated to have the most

similar P1 stem to the native riboswitch itself—predicted to have four base pairs by analogy to the *Eba* riboswitch (Figure S1C).

Because RNA contains many potential nonspecific sites for metal binding, and because the predicted apparent K_d ($K_{d,app}$) values are on the same order as the sensor concentrations,[43,50,51] we used 1 mM citrate to buffer the free concentration of metal ions in affinity titrations with Mn[II], Fe[II], Co[II], Ni[II], and Zn[II] to determine $K_{d,app}$ values. Interestingly, the *Lmo*-based sensors displayed a somewhat different selectivity pattern relative to the *Eba*-based **czcD** sensors. The **Lmo-1** (Figure 1C) and **Lmo-3** (Figure S1B)
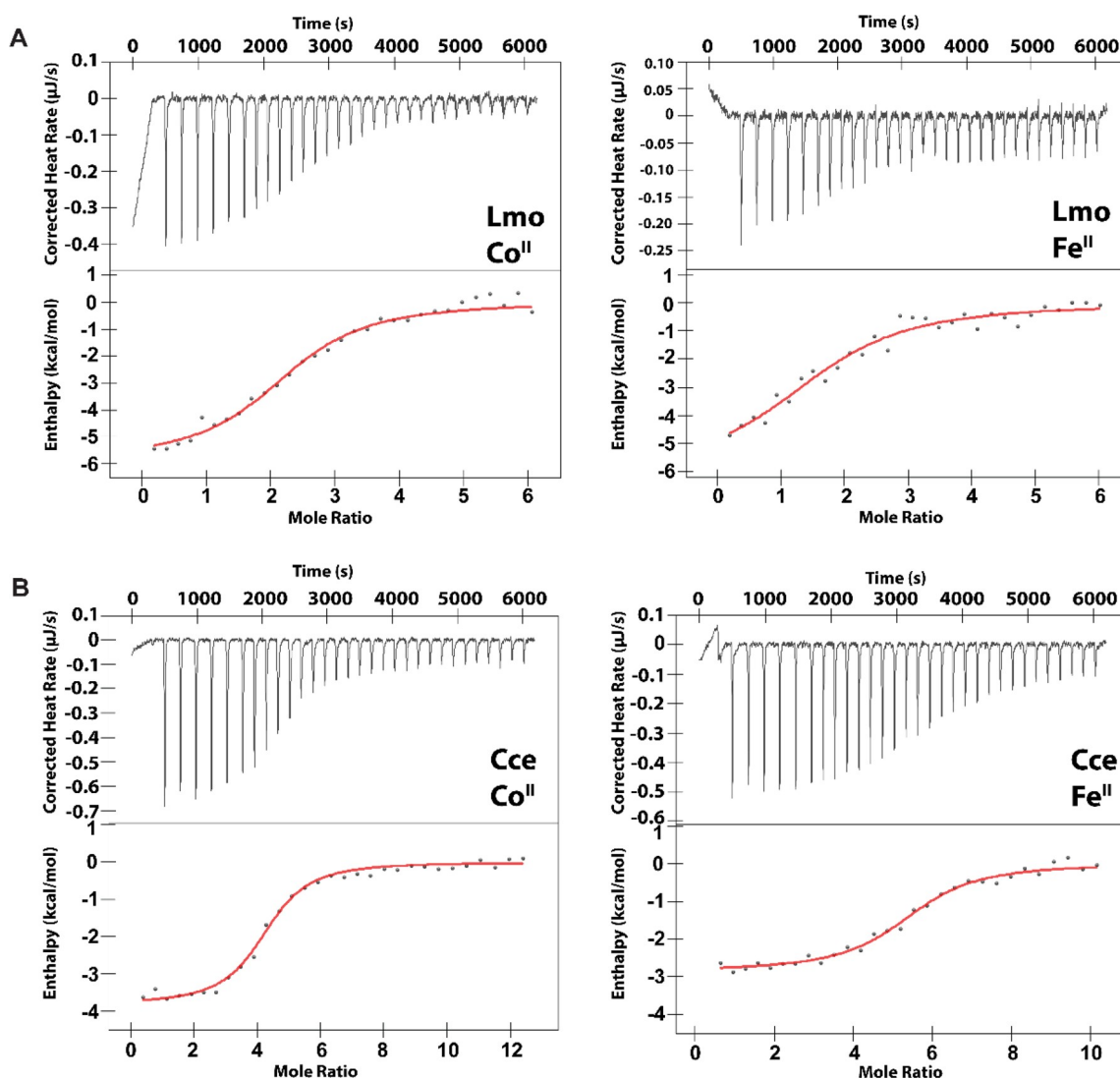
A

```
Eba      8    ---GAACUGAGCAGGCAAAUGACCAGAGCGGUCAUGCAGCC-GGGCUGCGAAAGCGGCAA    56
Sensei   1    GGUGGACGAAGUCGGCAGAGGUCCA---------UUAGUCGGGGCCGUAGUCACGGCAG    50
              *  **  **  ****  *   ***         **  * ****  *    *****
```

```
Eba      57   CAGAUGA-UUACACGCACAUCUGUGGGACAGUU    88
Sensei   51   CGGUUAUUUUAGAUCCACAACAGCCUAUCCC--    81
              *  *  *   *** *  **** *  *       *
```

B

Figure 3. Sensei RNA does not respond to iron. (A) Sequence alignment of the *Eba czcD* riboswitch and the *Hdu* Sensei RNA constructs used for ITC. The Sensei construct is the same one described by Ramesh and co-workers.[45] (B) ITC thermograms of *Hdu* Sensei (15 μM) titrated aerobically with 225 μM Co^{II} (left) and anaerobically with 225 μM Fe^{II} (right). The thermograms do not show evidence of significant metal binding and conformational change, beyond nonspecific interactions; compare Figures 2 and 4 for *czcD* riboswitches. Conditions: 30 mM MOPS, 100 mM KCl, 3 mM $MgCl_2$, pH 7.2, 20 °C.

constructs exhibited responses to Fe^{II}, Co^{II}, and Ni^{II} in accordance with the IW series, but no significant response to Mn^{II} and Zn^{II}. The **Lmo-2** sensor (Figure S1A) responded preferentially to Fe^{II}, Co^{II}, and Ni^{II}, but it also responded to Mn^{II} and Zn^{II}, albeit with higher $K_{d,app}$ values, as we had observed with **czcD-1**.[43] The Hill coefficients of all the sensors were 2 to 3, demonstrating similar cooperativity as the *Eba*-based sensors and suggesting that the attachment of the aptamer does not greatly perturb metal binding to the riboswitch. The results of the titrations are summarized in Table 1 (**Lmo-1**) and Tables S4 and S5 (**Lmo-2** and **Lmo-3**). The improved in vitro selectivity and fluorescence response of **Lmo-1** in particular suggests that it may perform more robustly in future bacterial imaging experiments than **czcD-2** did in our prior work. These studies suggest that the *Lmo* riboswitch may also be iron-responsive and show the generality of using the P1 stem to create fluorescent sensors based on *czcD* riboswitches, an observation that will be exploited below to probe the Sensei RNA.

Native *Eba czcD* Riboswitch Responds to Fe^{II} but Sensei Does Not

Whereas the riboswitch-based fluorescent sensors suggest that *czcD* riboswitches may respond to Fe^{II}, the specific $K_{d,app}$ values may be perturbed by fusion with the Spinach2 aptamer. Therefore, we used ITC to further characterize metal binding; this method allows extrapolation of thermodynamic parameters including K_d, stoichiometry (*n*), and enthalpy (ΔH) for metal binding and the accompanying conformational change.[52] We designed the ITC constructs by truncating the riboswitch at the P1 stem (Figure 1A, Table S1), similar to previous work on Mn^{II}-responsive riboswitches.[33,53] We first carried out

titrations of the *Eba czcD* riboswitch with Mn^{II}, Fe^{II}, Co^{II}, Ni^{II}, and Zn^{II} (Figures 2 and S2); the results are summarized in Table 2. The enthalpies associated with metal−*Eba* interactions are exothermic and similar in magnitude to those for Mn^{II}-responsive riboswitches (1−6 kcal/mol).[33,53] We assign the small residual heats observed at the end of all titrations (0.05−0.1 μJ/s) to nonspecific binding of the metal ions to the RNA.[33,53] In support of this assignment, the M3 variant of the *Eba* riboswitch, previously shown to ablate the RNA's conformational response,[44] exhibits background heats of the same magnitude but without the larger heat associated with a conformational response (Figure S3). *Eba* showed the highest-affinity interaction with Co^{II}, Ni^{II}, and Fe^{II}, with $K_{d,app}$ values of 0.5−1 μM. The $K_{d,app}$ values for Co^{II} and Ni^{II} binding are in good agreement with our fluorescent sensor studies[43] as well as values determined by Nesbitt and co-workers[54] and Unrau, Trachman, and co-workers[55] by independent methods, although those investigators did not study Fe^{II} binding. We note especially the quantitative agreement between our $K_{d,app}$ values and those of Nesbitt determined using single-molecule FRET, therefore supporting our interpretation that the observed enthalpy changes reflect the metal-induced conformational change. We were unable to detect any response with Mn^{II} (Figure S2), perhaps owing to a $K_{d,app}$ for Mn^{II}−*Eba* being significantly greater than the concentration of riboswitch used for this experiment. Simulation of ITC traces assuming *n* = 3, $\Delta H = -4.5$ kcal/mol, and [RNA] = 10 μM allows us to estimate that this $K_{d,app}$ value is 0.1−1 mM (Figure S4). Together, these results strongly suggest that Fe^{II} elicits a similar conformational response in the riboswitch as Co^{II} and Ni^{II}.

Figure 4. Representative thermograms from ITC studies of (A) *Lmo* and (B) *Cce czcD* riboswitches (8.2−9.9 μM RNA) with Co^{II} (left) or Fe^{II} (right). The data are fitted to a model with one set of equivalent binding sites. Fitted parameters are provided in Table 2. Conditions: 30 mM MOPS, 100 mM KCl, 3 mM $MgCl_2$, pH 7.2, 20 °C.

The metal-binding stoichiometry we observed for the *Eba* riboswitch contrasts with the four bound cobalt ions in the X-ray crystal structure of *Eba* determined by Furukawa et al. (Figure 1B).[44] As the fourth Co^{II} ion, C4 in Figure 1B, is only bound to one riboswitch nucleotide (G18) and exhibited lower occupancy than the others in the crystal structure, we hypothesized that its presence was an artifact of the high Co^{II} concentration (2 mM) in the crystallization condition. Therefore, we designed two new constructs of the riboswitch with the base pair G18−C44 on the P2 stem mutated to remove the G18 metal ligand, in order to investigate whether this change would perturb metal-binding stoichiometry. As the nonfunctional M3 variant is made by mutating two base pairs into mismatching guanines in the P2 stem,[44] the stability of this stem is important to the function of the riboswitch; therefore, we made mutations that will still retain the base pair at the G18−C44 positions: either CG (G18C/C44G, "*Eba*−CG") or UA (G18U/C44A, "*Eba*−UA"). In titrations with Co^{II}, we observed similar $K_{d,app}$ and *n* values compared to the wild-type riboswitch (Table 2, Figure S5). These results

suggest that the C4 site, in *Eba* at least, is not important for the riboswitch's conformational response.

Our ITC data contrast with the results of Ramesh and co-workers,[45] who reported little to no binding of Fe^{II} to *Eba* in equilibrium dialysis experiments. Conversely, their ITC analysis of the *Hdu* Sensei RNA indicated a K_d of 1.7 μM and 1:1 binding for Fe^{II}−Sensei, but no significant response to Co^{II}. Because Sensei and *czcD* were putatively structurally similar, we reasoned that a Sensei-based fluorescent sensor analogous to the several *czcD*-based sensors we have designed would allow us to investigate this apparent discrepancy. Therefore, we inserted the Spinach2 aptamer at the P1 stem of the *Hdu* Sensei RNA; the sequences of the resulting three constructs are provided in Table S1. We did not observe any fluorescence activation during citrate-buffered metal titrations, with Fe^{II} or Co^{II}, for any of the constructs (Figure S6). We also carried out ITC experiments with Fe^{II} and Co^{II} using the same *Hdu* Sensei RNA construct that was reported by Ramesh and co-workers; we did not observe a significant change in enthalpy, indicating that neither Fe^{II} nor Co^{II} induces a significant conformational change (Figure 3). After our work

was completed, Ramesh et al. retracted their paper, but the retraction notice left open the question of whether the Sensei RNA was an Fe^{II}-specific riboswitch. Our fluorescence and ITC results clearly demonstrate that it is not an Fe^{II}-responsive riboswitch.

Iron Responsiveness Is a General Property of *czcD* Riboswitches

Next, we assessed the *czcD* riboswitches from two other organisms, *Lmo* and *Cce*, in order to determine whether the iron responsiveness and overall thermodynamic parameters of the *Eba* riboswitch were representative for this riboswitch family. The *Lmo* riboswitch was selected for study because of our **Lmo** sensors (Figure 1C) and because we have shown the riboswitch-regulated ATPase, LMO3884, to rescue iron toxicity in *B. subtilis* when overexpressed.[43] *Cce* was selected because RT-qPCR studies of the riboswitch-regulated gene had been carried out in the initial report of the *czcD* riboswitches.[44] All three riboswitches have the metal-binding residues in the *Eba* X-ray structure fully conserved (Figure 1A). Characterization of the *Lmo* riboswitch (Figure 4A, Table 2, Figure S7) revealed a similar trend as with the *Eba* riboswitch, albeit with slightly higher $K_{d,app}$ values and a metal-binding stoichiometry of only ~2 for Fe^{II} and Co^{II}. The ITC data were also in good agreement with the **Lmo** fluorescent sensor results (Figure 1C, Table 1). By titrating Co^{II} and Fe^{II} into *Cce* (Figure 4B), we observed very similar metal–riboswitch affinities as with *Eba* and *Lmo* (Table 2). These results confirm that *Cce* is also a metal-responsive riboswitch. Interestingly, the stoichiometry for *Cce* is approximately 5, higher than the values observed for both *Eba* and *Lmo*. In all three cases, the response to Fe^{II} occurs with similar thermodynamic parameters, $K_{d,app}$, n, and ΔH as to Co^{II} and Ni^{II}. Therefore, these results emphasize the generality of iron responsiveness in the *czcD* riboswitch class.

Our ITC results establish that the *czcD* riboswitches bind and conformationally respond to Fe^{II}, just as they do to Co^{II} and Ni^{II} (as well as Zn^{II}, though with lower affinity). Despite conservation of the metal-binding nucleotides initially identified through the studies of Furukawa et al., these three riboswitches exhibit apparent differences in metal-binding stoichiometry. These differences may reflect the challenges of studying weak (micromolar affinity) metal-binding sites; nonspecific binding sites that are not linked to the conformational change may be of sufficiently similar affinity to the specific binding sites to affect the ITC stoichiometries. Nevertheless, all three *czcD* riboswitches bind at least two metal ions—suggesting that the two interconnected metal sites, C1 and C2 at the four-way junction (Figure 1B), may be the most critical for metal responsiveness and accounting for the cooperative binding observed in previous studies.[43,44,54] These results highlight how the rules for iron ligation by RNA are not yet understood, motivating future structural biology studies of iron-bound riboswitches.

The riboswitches' similar responsiveness to most of the divalent first-row transition metal ions motivates the question of which metal ion(s) is (are) physiologically relevant. The $K_{d,app}$ values for Fe^{II}–*czcD* complexes fall squarely within the range of characterized metalloregulatory proteins for Fe^{II}, such as *E. coli* and *S. enterica* Fur (1.2 μM[20] and 0.53 μM,[24] respectively) and even an Fe^{II}-chaperoning complex from *H. sapiens* (0.8 μM).[23] The $K_{d,app}$ values for Co^{II}–*czcD* complexes, however, are 1000-fold greater than for Co^{II}–RcnR (0.51 nM),[24] a model cobalt regulatory protein. The mismatches for

Ni^{II} (200 000-fold; 0.45 μM for Ni^{II}–*Eba* versus 2.5 pM for Ni^{II}–NikR) and Zn^{II} (4 000 000-fold; 2.7 μM for Zn^{II}–*Eba* versus 0.64 pM for Zn^{II}–Zur) are even more profound (Figure 5).[24] The differences in riboswitch/transcription factor $K_{d,app}$
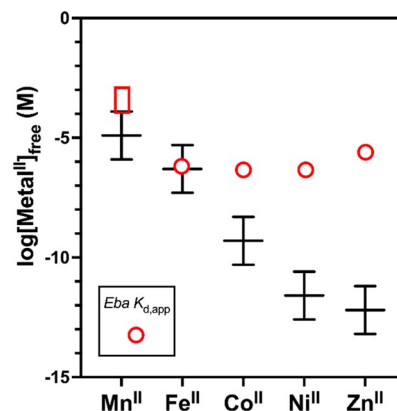
Figure 5. Comparison of $K_{d,app}$ values for response of the *Eba czcD* riboswitch to transition metal ions (open red box for Mn^{II}, open red circles for Fe^{II}, Co^{II}, Ni^{II}, and Zn^{II}) with the calculated ranges of intracellular labile metal ion concentrations (black lines) determined for the *Salmonella* model system.[24] The latter ranges consist of the free metal concentrations at which the relevant metal-sensing transcription factor gives 10, 50 (center), or 90% of its transcriptional response. Concept adapted from Young, Robinson, and co-workers,[25] with our data added. See http://creativecommons.org/licenses/by/4.0/ for license information. In the case of Mn^{II}, the red box indicates that the $K_{d,app}$ for the riboswitch is estimated to be 100−1000 μM (Figure S4). Because our experiments were carried out at 20 °C, but the prior ones were at 25 °C, our K_d values are slight underestimates relative to the intracellular labile metal ion concentrations. We also note that labile metal concentrations may differ somewhat from the *Salmonella* model, depending on the organism and aerobic versus anaerobic conditions.

values for Co^{II}, Ni^{II}, and Zn^{II} are even greater than was evident from the **czcD** fluorescent sensors.[43] Therefore, the riboswitches' $K_{d,app}$ values are well matched to those of iron regulatory proteins but not to the corresponding cobalt and nickel regulators that sense labile metal concentrations in cells. This observation argues that the most likely physiological function for the *czcD* riboswitches is to sense iron.

■ DISCUSSION

Our results demonstrate that the *czcD* riboswitches from three different organisms respond to Fe^{II}, Co^{II}, and Ni^{II} with similar dissociation constants in the 1 μM range. Interestingly, this conclusion differs somewhat from that based on analysis of riboswitch-derived fluorescent sensors,[43] which exhibited responses with greater metal dependence, in accordance with the Irving-Williams series. The native *czcD* riboswitches have flattened the typical affinity trend, with the exception of Mn^{II} (Figure 5). Viewing this trend in the context of buffered labile metal ion concentrations (see Introduction), with Fe^{II} and Mn^{II} being regulated in similar ranges, we hypothesize that the riboswitch is primarily tuned to suppress responsiveness to physiological concentrations of Mn^{II} and, as a result, is less selective for Fe^{II} against Co^{II} and Ni^{II} (and Zn^{II}). Presumably, however, the potential response to Co^{II} and Ni^{II}, not just to Fe^{II}, is mitigated in vivo, because the labile concentrations of Co^{II} and Ni^{II} are buffered by intracellular protein and small-molecule ligands and regulated at labile concentrations below

that which is necessary to induce a response from the riboswitch, except when confronted with the highest levels of metal stress.[24,25]

Of course, it is necessary to obtain explicit in vivo information about *czcD*'s metal selectivity, which is a focus of our current efforts. Nevertheless, indirect in vivo information is currently available to support our argument. Wang et al. recently reported that an mCherry transcriptional reporter regulated by the *czcD* riboswitch requires 50 μM Co^{II} or at least 1 mM Ni^{II} added to rich media (LB) in order to observe a significant response in *E. coli*.[56] This result is in line with the increasing discrepancy between intracellular buffered metal concentration and the metal−*czcD* K_d value (Figure 5) from Fe^{II} to Co^{II} to Ni^{II}, suggesting that response to Ni^{II} would only be relevant under the most extreme conditions. Furthermore, although Wang et al. did not assess whether their reporter was responding to basal iron levels, the **czcD-2** sensor, with a K_d (0.4 μM) for Fe^{II} similar to that of the native riboswitch (1.0 μM), did show a basal response to Fe^{II} even in minimal media with no added iron.[43] Therefore, whereas we cannot rule out the possibility that in some organisms or under certain conditions other metals (primarily Co^{II})[44] might be able to transiently induce an aberrant response,[27] our results herein clarify that the *czcD* riboswitch's selectivity seems to be well tuned for iron when examined in the cellular context, and we hypothesize that iron is the primary ligand for the *czcD* riboswitches.

Having established *czcD* as the only known family of iron-responsive riboswitches, next we consider potential roles of these riboswitches and the genes that they regulate. Many of the predicted *czcD* riboswitches are present upstream of putative metal-effluxing P$_{1B4}$-type ATPases.[44] The identification of the primary substrate of this family of ATPases has long been contentious; while many can transport Co^{II} under certain conditions,[57,58] recent work has revealed that the physiological function of at least some of these ATPases is iron detoxification.[38−40] It remains to be determined whether this function is shared by the riboswitch-regulated P$_{1B4}$-type ATPases, although results in a heterologous system suggest that the riboswitch-regulated *Lmo* P$_{1B4}$ ATPase LMO3448 exports iron efficiently.[43] This gene also has been recently shown to be induced by lactic acid stress, by an unknown mechanism.[59] In other organisms, the association between metal excess and the riboswitch-regulated genes is less clear. The Ccel_1038 gene positively regulated by the riboswitch in *Cce* is annotated as an MgtA-like P$_3$-type ATPase. In *E. coli* and *Salmonella enterica* serovar Typhimurium, MgtA is an *importer* of Mg^{II}, and the activity of the purified enzyme is inhibited by Co^{II}, Ni^{II}, and Zn^{II} (Fe^{II} was not tested).[60] This connection suggests that high levels of iron may interfere with magnesium homeostasis in *Cce*, leading to increased expression of a riboswitch-regulated Mg^{II} importer as a compensatory mechanism. We note that prediction of direction of transport and metal selectivity in P-type ATPases is not trivial and sometimes controversial;[61,62] therefore, determination of whether these annotated *mgtA* genes indeed encode Mg^{II} importers will require additional investigation. In still other organisms, the genes putatively regulated by this class of riboswitch do not seem to be ATPases at all, suggesting an even broader array of cellular physiology that might be impacted by iron levels. Detailed examination of these systems promises to shed significant light on the mechanisms and consequences of iron overload in a multitude of bacteria.

Lmo strains possessing the riboswitch might yield particular insight into its function. *Listeriaceae* encode a chromosomal P$_{1B4}$ ATPase, FrvA (LMO0641), that is regulated by Fur and the iron-dependent hydrogen peroxide sensor PerR and is implicated in iron efflux in response to iron overload, at least under aerobic conditions.[39,41] Many clinical and environmental isolates, but not wild-type *Listeria* strains like EGD-e, also possess an accessory plasmid that contains the riboswitch-regulated P$_{1B4}$ ATPase mentioned above, LMO3448 (42% sequence identity with FrvA).[44,59,63] Why two seemingly redundant ATPases with different regulatory mechanisms exist in these strains remains to be explored, but the redundancy might suggest the particular importance of defending against iron excess. For example, the riboswitch-mediated mechanism might enable a more rapid response to iron excess; alternatively, the two regulatory mechanisms might be tuned to respond at slightly different labile iron levels. The K_d of the *Lmo* riboswitch (2.2 μM) is slightly higher than the K_ds of the *Eba* and *Cce* riboswitches (1 μM), which are more similar to the K_d of *E. coli* Fe^{II}−Fur (1.2 μM).[20] Perhaps most intriguingly, the riboswitch and its downstream P$_{1B4}$ ATPase may provide a mechanism for sensing and responding to iron excess specifically under anaerobic conditions, when PerR may not be active. This proposal is supported by the observation that all bacteria containing *czcD* are either obligate or facultative anaerobes; furthermore, labile Fe^{II} levels would likely be higher in anaerobiosis than in aerobiosis,[64] which might account for the higher Fe^{II}−riboswitch K_d value. We are currently interrogating the riboswitch's place in *Listeriaceae* metallophysiology.

■ CONCLUSIONS

We have demonstrated that three native *czcD* riboswitches respond to Fe^{II} with $K_d \sim 1$ μM, with similar affinities for Co^{II}, Ni^{II}, and Zn^{II}. Consideration of these results in the context of cellular metal regulation suggests that the riboswitch is tuned to preferentially respond to Fe^{II} in vivo. By contrast, our studies of the Sensei RNA indicate that it is not an iron-responsive riboswitch. We propose that the primary physiological function of *czcD* riboswitches is to respond to high iron levels, and in vivo investigations are in progress to test this hypothesis.

■ ASSOCIATED CONTENT

ⓈⒾ Supporting Information

The Supporting Information is available free of charge at https://pubs.acs.org/doi/10.1021/acsbiomedche-mau.1c00069.

> Supplemental tables (including RNA constructs, primers, and titration data) and figures (additional fluorescence and ITC data) (PDF)

Accession Codes

Eba3544, Uniprot entry E2SQM5; LMO3448, Uniprot entry T1YRD8; Ccel_1038, Uniprot entry B8I9E0; FrvA, Uniprot entry Q8Y992.

■ AUTHOR INFORMATION

Corresponding Author

Joseph A. Cotruvo, Jr. − *Department of Chemistry, The Pennsylvania State University, University Park, Pennsylvania 16802, United States; Center for RNA Molecular Biology,*

The Pennsylvania State University, University Park, Pennsylvania 16802, United States; ● orcid.org/0000-0003-4243-8257; Email: juc96@psu.edu

Author

Jiansong Xu − *Department of Chemistry, The Pennsylvania State University, University Park, Pennsylvania 16802, United States; Center for RNA Molecular Biology, The Pennsylvania State University, University Park, Pennsylvania 16802, United States;* ● orcid.org/0000-0002-2708-2996

Complete contact information is available at:
https://pubs.acs.org/10.1021/acsbiomedchemau.1c00069

Notes

The authors declare no competing financial interest.

■ REFERENCES

(1) Barge, L. M.; Flores, E.; Baum, M. M.; VanderVelde, D. G.; Russell, M. J. Redox and pH gradients drive amino acid synthesis in iron oxyhydroxide mineral systems. *Proc. Natl. Acad. Sci. U. S. A.* **2019**, *116*, 4828−4833.

(2) Lin, S.-Y.; Wang, Y.-C.; Hsiao, C. Prebiotic iron originates the peptidyl transfer origin. *Mol. Biol. Evol.* **2019**, *36*, 999−1007.

(3) Muchowska, K. B.; Varma, S. J.; Moran, J. Synthesis and breakdown of universal metabolic precursors promoted by iron. *Nature* **2019**, *569*, 104−107.

(4) Guth-Metzler, R.; Bray, M. S; Frenkel-Pinter, M.; Suttapitugsakul, S.; Montllor-Albalate, C.; Bowman, J. C; Wu, R.; Reddi, A. R; Okafor, C D.; Glass, J. B; Williams, L. D. Cutting in-line with iron: ribosomal function and non-oxidative RNA cleavage. *Nucleic Acids Res.* **2020**, *48*, 8663−8674.

(5) Hsiao, C.; Chou, I. C.; Okafor, C. D.; Bowman, J. C.; O'Neill, E. B.; Athavale, S. S.; Petrov, A. S.; Hud, N. V.; Wartell, R. M.; Harvey, S. C.; Williams, L. D. RNA with iron(II) as a cofactor catalyses electron transfer. *Nat. Chem.* **2013**, *5*, 525−528.

(6) Okafor, C. D.; Lanier, K. A.; Petrov, A. S.; Athavale, S. S.; Bowman, J. C.; Hud, N. V.; Williams, L. D. Iron mediates catalysis of nucleic acid processing enzymes: support for Fe(II) as a cofactor before the great oxidation event. *Nucleic Acids Res.* **2017**, *45*, 3634−3642.

(7) Lill, R.; Freibert, S.-A. Mechanisms of mitochondrial iron-sulfur protein biogenesis. *Annu. Rev. Biochem.* **2020**, *89*, 471−499.

(8) Talib, E. A.; Outten, C. E. Iron-sulfur cluster biogenesis, trafficking, and signaling: Roles for CGFS glutaredoxins and BolA proteins. *Biochim. Biophys. Acta - Mol. Cell Res.* **2021**, *1868*, 118847.

(9) Chambers, I. G.; Willoughby, M. M.; Hamza, I.; Reddi, A. R. One ring to bring them all and in the darkness bind them: The trafficking of heme without deliverers. *Biochim. Biophys. Acta - Mol. Cell Res.* **2021**, *1868*, 118881.

(10) Krebs, C.; Galonić Fujimori, D.; Walsh, C. T.; Bollinger, J. M. Non-heme Fe(IV)−oxo intermediates. *Acc. Chem. Res.* **2007**, *40*, 484−492.

(11) Posey, J. E.; Gherardini, F. C. Lack of a role for iron in the Lyme disease pathogen. *Science* **2000**, *288*, 1651−1653.

(12) Lee, J. W.; Helmann, J. D. The PerR transcription factor senses H_2O_2 by metal-catalysed histidine oxidation. *Nature* **2006**, *440*, 363−367.

(13) Sobota, J. M.; Imlay, J. A. Iron enzyme ribulose-5-phosphate 3-epimerase in *Escherichia coli* is rapidly damaged by hydrogen peroxide but can be protected by manganese. *Proc. Natl. Acad. Sci. U.S.A.* **2011**, *108*, 5402−5407.

(14) Imlay, J. A. The mismetallation of enzymes during oxidative stress. *J. Biol. Chem.* **2014**, *289*, 28121−28128.

(15) Chandrangsu, P.; Rensing, C.; Helmann, J. D. Metal homeostasis and resistance in bacteria. *Nat. Rev. Microbiol.* **2017**, *15*, 338−350.

(16) Ma, Z.; Jacobsen, F. E.; Giedroc, D. P. Coordination chemistry of bacterial metal transport and sensing. *Chem. Rev.* **2009**, *109*, 4644−4681.

(17) Helmann, J. D. Specificity of metal sensing: iron and manganese homeostasis in *Bacillus subtilis*. *J. Biol. Chem.* **2014**, *289*, 28112−28120.

(18) Foster, A. W.; Young, T. R.; Chivers, P. T.; Robinson, N. J. Protein metalation in biology. *Curr. Opin. Chem. Biol.* **2022**, *66*, 102095.

(19) Keyer, K.; Imlay, J. A. Superoxide accelerates DNA damage by elevating free-ironlevels. *Proc. Natl. Acad. Sci. U.S.A.* **1996**, *93*, 13635−13640.

(20) Mills, S. A.; Marletta, M. A. Metal binding characteristics and role of iron oxidation in the ferric uptake regulator from *Escherichia coli*. *Biochemistry* **2005**, *44*, 13553−13559.

(21) Guedon, E.; Helmann, J. D. Origins of metal ion selectivity in the DtxR/MntR family of metalloregulators. *Mol. Microbiol.* **2003**, *48*, 495−506.

(22) Cassat, J. E.; Skaar, E. P. Iron in infection and immunity. *Cell Host Microbe* **2013**, *13*, 509−519.

(23) Patel, S. J.; Frey, A. G.; Palenchar, D. J.; Achar, S.; Bullough, K. Z.; Vashisht, A.; Wohlschlegel, J. A.; Philpott, C. C. A PCBP1-BolA2 chaperone complex delivers iron for cytosolic [2Fe-2S] cluster assembly. *Nat. Chem. Biol.* **2019**, *15*, 872−881.

(24) Osman, D.; Martini, M. A.; Foster, A. W.; Chen, J.; Scott, A. J. P.; Morton, R. J.; Steed, J. W.; Lurie-Luke, E.; Huggins, T. G.; Lawrence, A. D.; Deery, E.; Warren, M. J.; Chivers, P. T.; Robinson, N. J. Bacterial sensors define intracellular free energies for correct enzyme metalation. *Nat. Chem. Biol.* **2019**, *15*, 241−249.

(25) Young, T. R.; Martini, M. A.; Foster, A. W.; Glasfeld, A.; Osman, D.; Morton, R. J.; Deery, E.; Warren, M. J.; Robinson, N. J. Calculating metalation in cells reveals CobW acquires Co^{II} for vitamin B$_{12}$ biosynthesis while related proteins prefer Zn^{II}. *Nat. Commun.* **2021**, *12*, 1195.

(26) Irving, H.; Williams, R. J. P. Order of stability of metal complexes. *Nature* **1948**, *162*, 746−747.

(27) Osman, D.; Foster, A. W.; Chen, J.; Svedaite, K.; Steed, J. W.; Lurie-Luke, E.; Huggins, T. G.; Robinson, N. J. Fine control of metal concentrations is necessary for cells to discern zinc from cobalt. *Nat. Commun.* **2017**, *8*, 1884.

(28) Mandal, M.; Breaker, R. R. Gene regulation by riboswitches. *Nat. Rev. Mol. Cell Biol.* **2004**, *5*, 451−463.

(29) McCown, P. J.; Corbino, K. A.; Stav, S.; Sherlock, M. E.; Breaker, R. R. Riboswitch diversity and distribution. *RNA* **2017**, *23*, 995−1011.

(30) Dann, C. E.; Wakeman, C. A.; Sieling, C. L.; Baker, S. C.; Irnov, I.; Winkler, W. C. Structure and mechanism of a metal-sensing regulatory RNA. *Cell* **2007**, *130*, 878−892.

(31) Price, I. R.; Gaballa, A.; Ding, F.; Helmann, J. D.; Ke, A. Mn^{2+}-sensing mechanisms of *yybP-ykoY* orphan riboswitches. *Mol. Cell* **2015**, *57*, 1110−1123.

(32) Dambach, M.; Sandoval, M.; Updegrove, T. B.; Anantharaman, V.; Aravind, L.; Waters, L. S.; Storz, G. The ubiquitous *yyb-ykoY* riboswitch is a manganese-responsive regulatory element. *Mol. Cell* **2015**, *57*, 1099−1109.

(33) Martin, J. E.; Le, M. T.; Bhattarai, N.; Capdevila, D. A.; Shen, J.; Winkler, M. E.; Giedroc, D. P. A Mn-sensing riboswitch activates expression of a Mn^{2+}/Ca^{2+} ATPase transporter in *Streptococcus*. *Nucleic Acids Res.* **2019**, *47*, 6885−6899.

(34) Massé, E.; Gottesman, S. A small RNA regulates the expression of genes involved in iron metabolism in *Escherichia coli*. *Proc. Natl. Acad. Sci. U.S.A.* **2002**, *99*, 4620−4625.

(35) Frawley, E. R.; Fang, F. C. The ins and outs of bacterial iron metabolism. *Mol. Microbiol.* **2014**, *93*, 609−616.

(36) Pi, H.; Helmann, J. D. Ferrous iron efflux systems in bacteria. *Metallomics* **2017**, *9*, 840−851.

(37) Brown, J. B.; Lee, M. A.; Smith, A. T. Ins and outs: Recent advancements in membrane protein-mediated prokaryotic ferrous iron transport. *Biochemistry* **2021**, *60*, 3277−3291.

(38) Guan, G.; Pinochet-Barros, A.; Gaballa, A.; Patel, S. J.; Argüello, J. M.; Helmann, J. D. PfeT, a P_{1B4}-type ATPase, effluxes ferrous iron and protects *Bacillus subtilis* against iron intoxication. *Mol. Microbiol.* **2015**, *98*, 787−803.

(39) Pi, H.; Patel, S. J.; Argüello, J. M.; Helmann, J. D. The *Listeria monocytogenes* Fur-regulated virulence protein FrvA is an Fe(II) efflux P_{1B4}-type ATPase. *Mol. Microbiol.* **2016**, *100*, 1066−1079.

(40) Patel, S. J.; Lewis, B. E.; Long, J. E.; Nambi, S.; Sassetti, C. M.; Stemmler, T. L.; Argüello, J. M. Fine-tuning of substrate affinity leads to alternative roles of *Mycobacterium tuberculosis* Fe^{2+}-ATPases. *J. Biol. Chem.* **2016**, *291*, 11529−11539.

(41) Pinochet-Barros, A.; Helmann, J. D. *Bacillus subtilis* Fur is a transcriptional activator for the PerR-repressed *pfeT* gene, encoding an iron efflux pump. *J. Bacteriol.* **2020**, *202*, No. e00697-19.

(42) Ma, J.; Haldar, S.; Khan, M. A.; Sharma, S. D.; Merrick, W. C.; Theil, E. C.; Goss, D. J. Fe^{2+} binds iron responsive element-RNA, selectively changing protein-binding affinities and regulating mRNA repression and activation. *Proc. Natl. Acad. Sci. U.S.A.* **2012**, *109*, 8417−8422.

(43) Xu, J.; Cotruvo, J. A., Jr. The *czcD* (NiCo) riboswitch responds to iron(II). *Biochemistry* **2020**, *59*, 1508−1516.

(44) Furukawa, K.; Ramesh, A.; Zhou, Z.; Weinberg, Z.; Vallery, T.; Winkler, W. C.; Breaker, R. R. Bacterial riboswitches cooperatively bind Ni^{2+} or Co^{2+} ions and control expression of heavy metal transporters. *Mol. Cell* **2015**, *57*, 1088−1098.

(45) Bandyopadhyay, S.; Chaudhury, S.; Mehta, D.; Ramesh, A. RETRACTED ARTICLE: Discovery of iron-sensing bacterial riboswitches. *Nat. Chem. Biol.* **2021**, *17*, 924.

(46) Kellenberger, C. A.; Wilson, S. C.; Sales-Lee, J.; Hammond, M. C. RNA-based fluorescent biosensors for live cell imaging of second messengers cyclic di-GMP and cyclic AMP-GMP. *J. Am. Chem. Soc.* **2013**, *135*, 4906−4909.

(47) You, M.; Litke, J. L.; Jaffrey, S. R. Imaging metabolite dynamics in living cells using a Spinach-based riboswitch. *Proc. Natl. Acad. Sci. U.S.A.* **2015**, *112*, E2756−E2765.

(48) Wang, X. C.; Wilson, S. C.; Hammond, M. C. Next-generation RNA-based fluorescent biosensors enable anaerobic detection of cyclic di-GMP. *Nucleic Acids Res.* **2016**, *44*, No. e139.

(49) Song, W.; Strack, R. L.; Svensen, N.; Jaffrey, S. R. Plug-and-play fluorophores extend the spectral properties of Spinach. *J. Am. Chem. Soc.* **2014**, *136*, 1198−1201.

(50) Xiao, Z.; Wedd, A. G. The challenges of determining metal-protein affinities. *Nat. Prod. Rep.* **2010**, *27*, 768−789.

(51) Young, T. R.; Xiao, Z. Principles and practice of determining metal−protein affinities. *Biochem. J.* **2021**, *478*, 1085−1116.

(52) Jones, C. P.; Piszczek, G.; Ferré-D'Amaré, A. R. Isothermal titration calorimetry measurement of riboswitch-ligand interactions. *Microcalorimetry of Biological Molecules: Methods and Protocols* **2019**, *1964*, 75−87.

(53) Bachas, S. T.; Ferré-D'Amaré, A. R. Convergent use of heptacoordination for cation selectivity by RNA and protein metalloregulators. *Cell Chem. Biol.* **2018**, *25*, 962−973 e5.

(54) Sung, H.-L.; Nesbitt, D. J. Sequential folding of the nickel/cobalt riboswitch is facilitated by a conformational intermediate: Insights from single-molecule kinetics and thermodynamics. *J. Phys. Chem. B* **2020**, *124*, 7348−7360.

(55) Jeng, S. C. Y.; Trachman, R. J.; Weissenboeck, F.; Truong, L.; Link, K. A.; Jepsen, M. D. E.; Knutson, J. R.; Andersen, E. S.; Ferré-D'Amaré, A. R.; Unrau, P. J. Fluorogenic aptamers resolve the flexibility of RNA junctions using orientation-dependent FRET. *RNA* **2021**, *27*, 433−444.

(56) Wang, X.; Wei, W.; Zhao, J. Using a riboswitch sensor to detect Co^{2+}/Ni^{2+} transport in *E. coli*. *Front. Chem.* **2021**, *9*, 631909.

(57) Zielazinski, E. L.; Cutsail, G. E., III; Hoffman, B. M.; Stemmler, T. L.; Rosenzweig, A. C. Characterization of a cobalt-specific P_{1B}-ATPase. *Biochemistry* **2012**, *51*, 7891−900.

(58) Raimunda, D.; Long, J. E.; Padilla-Benavides, T.; Sassetti, C. M.; Argüello, J. M. Differential roles for the Co^{2+}/Ni^{2+} transporting ATPases, CtpD and CtpJ, in *Mycobacterium tuberculosis* virulence. *Mol. Microbiol.* **2014**, *91*, 185−197.

(59) Cortes, B. W.; Naditz, A. L.; Anast, J. M.; Schmitz-Esser, S. Transcriptome sequencing of *Listeria monocytogenes* reveals major gene expression changes in response to lactic acid stress exposure but a less pronounced response to oxidative stress. *Front. Microbiol.* **2020**, *10*, 3110.

(60) Subramani, S.; Perdreau-Dahl, H.; Morth, J. P. The magnesium transporter A is activated by cardiolipin and is highly sensitive to free magnesium in vitro. *eLife* **2016**, *5*, No. e11407.

(61) Smith, A. T.; Smith, K. P.; Rosenzweig, A. C. Diversity of the metal-transporting P_{1B}-type ATPases. *J. Biol. Inorg. Chem.* **2014**, *19*, 947−960.

(62) Lewinson, O.; Lee, A. T.; Rees, D. C. A P-type ATPase importer that discriminates between essential and toxic transition metals. *Proc. Natl. Acad. Sci. U.S.A.* **2009**, *106*, 4677−4682.

(63) LeBrun, M.; Loulergue, J.; Chaslus-Dancla, E.; Audurier, A. Plasmids in *Listeria monocytogenes* in relation to cadmium resistance. *Appl. Environ. Microbiol.* **1992**, *58*, 3183−3186.

(64) Beauchene, N. A.; Mettert, E. L.; Moore, L. J.; Keleş, S.; Willey, E. R.; Kiley, P. J. O_2 availability impacts iron homeostasis in *Escherichia coli*. *Proc. Natl. Acad. Sci. U.S.A.* **2017**, *114*, 12261−12266.